Proceedings of the 2006 IEEE/RSJ
International Conference on Intelligent Robots and Systems
October 9 - 15, 2006, Beijing, China

Turning Maneuvers of a Multi-legged Modular Robot Using Its Inherent Dynamic Characteristics

Shinya Aoi, Hitoshi Sasaki, and Kazuo Tsuchiya
Dept. of Aeronautics and Astronautics, Graduate School of Engineering, Kyoto University
Yoshida-honmachi, Sakyo-ku, Kyoto 606-8501, Japan
Email: {shinya_aoi, tsuchiya}@kuaero.kyoto-u.ac.jp

Abstract— **This paper deals with the motion of a multi-legged modular robot. The robot consists of six homogenous modules, each of which has a body and two legs and is connected to the others through a three-degree-of-freedom joint. The leg joints are manipulated to follow periodic desired trajectories, and the joints between the modules act like a passive spring with a damper. This robot has characteristic dynamic properties. Specifically, a straight walk naturally turns into a meandering walk by changing the compliance of the joints between the modules without incorporation of any oscillatory inputs. We first show that this transition is excited due to a Hopf bifurcation, based on a numerical simulation and Floquet analysis. Following that, we examine whether the maneuverability and agility increase by utilizing the dynamic characteristics inherent in the robot. In particular, we conduct an experiment in which the robot pursues a target moving across the floor. We propose a simple controller to accomplish the task and achieve high maneuverability and agility by making the most of the robot's dynamic features.**

I. Introduction

Modular robots consist of a set of robotic modules that change the configuration and strength of their connection, which allows them to deal with a wide variety of tasks. In the literatures, many modular robots have been developed that have capabilities such as self-reconfiguration, fault tolerance, and locomotion [6], [10], [35], [36]. In particular, legged-type modular robots, which are specialized for locomotion, have high possibility to move across uneven terrain and high adaptability to various environments [18], [19], [31]. They are expected to display their great ability in a lot of places.

However, we still have many difficulties to achieve sophisticated legged robots and their control system. In particular, 1) the robot is a mechanical system with many degrees of freedom, composed of many links that are connected with others by joints, some of which are redundant in achieving its walking. The essential problem is how to coordinate their motions; 2) the leg motion consists of the swing and stance phases. The swing leg lands on the ground and in turn becomes the stance leg. Therefore, periodically and intermittently, the legs receive reaction forces from the ground. In other words, the condition of foot-to-ground contact is changeable, resulting in changes of the dynamics that governs the walking motion and influencing the walking stability. To overcome these difficulties, studies have been widely carried out based on the model-based approach [5], [16]. In this approach, the robot motion is basically generated by the inverse kinematics and kinetics, for example, by calculating the foot landing positions to keep the walk stable and then computing the joint motions. However, complicated computations are required, as are precise modeling of the robot and environment, which restricts the possibility of attaining adaptability and robustness. In addition to these difficulties, a robot that possesses many legs has the following characteristic problem: since its many legs are in contact with the ground and support the robot, they keep the robot from falling over. However, all those contact legs also keep the robot from accomplishing maneuverable and agile motions such as a quick turn. Therefore, it is difficult to simply design a locomotion control system and achieve high adaptability and maneuverability of the robot motion.

This is contrast to the millions of animal species that adapt themselves to various environments by manipulating their complicated and redundant musculoskeletal system, giving them marvelous maneuverability and agility. Recently, many researchers have developed biologically inspired robots and aimed to clarify the control mechanisms of animals. Especially, neurophysiological studies have revealed that animal walking is generated by a central pattern generator (CPG) [17], [23]. A CPG comprises a set of neural oscillators present in the spinal cord, spontaneously generating rhythmic signals that activate their limbs. The CPG modulates signal generation in response to the sensory signals, resulting in adaptive motions. The CPG is widely modeled using nonlinear oscillators [28], and based on such CPG models many locomotion robots and their control systems have been developed [2], [4], [8], [11], [18], [22]. Also from the field of neurophysiology, it has been revealed that, as well as rhythm control, muscle tone control has an important role in generating adaptive motions [21], [29], suggesting the importance of compliance in locomotion. Actually, many studies on robotics demonstrated the essential roles of the compliance. Specifically, by appropriately employing the mechanical compliance, simple control systems attained highly adaptive, robust, and agile motions, especially in hexapod robots [7], [9], [25], quadruped robots [11], [24], and biped robots [30], [34].

Animals generate their motions by skillfully applying the intrinsic characteristics of their musculoskeletal system. In particular, many researchers have used simple models and analyzed self-stabilizing properties embedded in their musculoskeletal system that indicates to accomplish stable motions without depending on external sensors [14], [15], [26], [33]. As well as with animals, many studies have been carried out to elucidate such self-stabilization inherent in locomotion robots also by employing simple models [1], [3], [13].

1-4244-0259-X/06/$20.00 ©2006 IEEE

Dynamic characteristics such as stability must strongly affect the maneuverability and agility of locomotion. For example, cockroaches are highly agile and have a great range of maneuverability [12], [20]. Schmitt and Holmes [26], [27] simply modeled the hexapod walking of a cockroach, and then analytically demonstrated that it successfully achieves a quick turn by virtue of destabilizing its straight walking motion by changing its dynamic features. It would be very interesting and helpful if we attained such maneuverability and agility of locomotion robots by using the dynamic properties inherent in the robots.

In this paper, we deal with a multi-legged modular robot composed of six homogenous modules and in particular we study its rudimentary locomotion. Each module has two legs and the modules are connected to each other through a three-degree-of-freedom (DOF) rotary joint. The robot has a simple controller that generates periodic leg trajectories. The leg joints are manipulated to follow periodic desired trajectories and each joint between modules acts like a passive spring with a damper. This robot features characteristic dynamic properties. Specifically, a straight walk by the robot naturally turns into a meandering walk by changing the strength of the connection between the modules without actually incorporating any oscillatory inputs. That is, the dynamic stability of a straight walk varies depending on the compliance of the joints between the modules. We show that the transition from a straight to a meandering walk is excited due to a Hopf bifurcation, based on a numerical simulation and Floquet analysis.

As described above, it is difficult for a locomotion robot that has many legs to achieve agile motions such as a quick turn because of the contact legs and motion planning. Since such a motion is a fundamental behavior for a locomotion robot, its dynamic characteristics should be thoroughly analyzed and the problem should be solved. Although the model-based approach is generally used, it requires precise modeling and complicated computations, preventing from achieving adaptive locomotion and simple control system. In this paper, we especially focus on the dynamic characteristics embedded in the multi-legged modular robot as one of the solutions to the problem. In particular, we investigate whether the maneuverability and agility of the robot increase by using the dynamic characteristics. We conduct an experiment in which the robot pursues a target moving across the floor. We then propose a simple controller to accomplish the task and achieve high maneuverability and agility by making the most of the robot's dynamic features.

II. A Multi-legged Modular Robot

A. Robot Model

Figure 1 shows a schematic diagram of the multi-legged modular robot considered in this paper. The robot has six homogenous modules, each with one body and two legs. Each leg consists of three links that are connected to each other through a one-DOF rotational joint (see Fig. 2). The legs are articulated to the body also by a one-DOF rotational joint. Each module is connected to the next through a coupler composed of roll, pitch, and yaw joints, with each joint

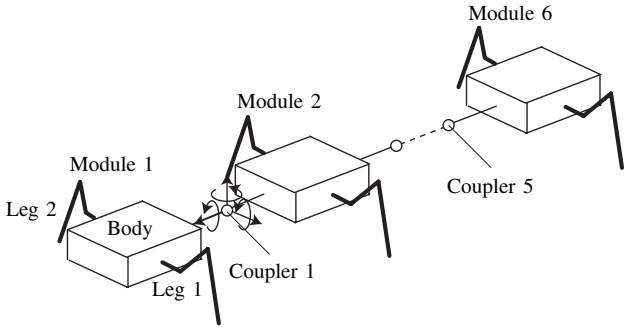

Fig. 1. Schematic model of a multi-legged modular robot

manipulated by a motor. The modules are enumerated from Module 1 to Module 6, and the coupler between Module i and Module $(i+1)$ is numbered Coupler i ($i = 1, \ldots, 5$). The left and right legs are numbered Legs 1 and 2, respectively. The joints and links of each leg are numbered from the side of the body as Joints 1, 2, and 3 and Links 1, 2, and 3, respectively. The position vector of the body of Module 1 is given by vector $[\, x_1 \, x_2 \, x_3 \,]$ expressed on the ground, where x_1 and x_3 are toward the nominal direction of locomotion and the vertical direction, respectively. The posture of the body of Module 1 is given by Euler angles $[\, \theta_{11} \, \theta_{12} \, \theta_{13} \,]$, where θ_{11}, θ_{12}, and θ_{13} correspond to roll, pitch, and yaw angles, respectively. Similarly, angles θ_{im} ($i = 2, \ldots, 6$, $m = 1, 2, 3$) are the components of relative angles of Module i with respect to Module $(i-1)$, which correspond to the angles of Coupler $(i-1)$. Angles θ_{ik}^{j} ($i = 1, \ldots, 6$, $j = 1, 2$, $k = 1, 2, 3$) are the relative angles of Joint k of Leg j of Module i.

State variable $q \in \mathbb{R}^{57}$ is defined as $q^{\mathrm{T}} = [\, x_m \, \theta_{im} \, \theta_{ik}^{j} \,]$ ($i = 1, \ldots, 6$, $j = 1, 2$, $k = 1, 2, 3$, $m = 1, 2, 3$). An equation of motion for the state variable is derived using Lagrangian formulation by

$$M(q)\ddot{q} + H(q, \dot{q}) = G(q) + U + \Lambda \tag{1}$$

where $M(q) \in \mathbb{R}^{57 \times 57}$ is the inertia matrix, $H(q, \dot{q}) \in \mathbb{R}^{57}$ is the nonlinear term that includes Coriolis and centrifugal forces, $G(q) \in \mathbb{R}^{57}$ is the gravity term, $U \in \mathbb{R}^{57}$ is the input torque term, and Λ is the reaction force from the ground. The ground is modeled as a spring with a damper in the vertical direction and a viscous damper in the horizontal direction. In this paper, numerical simulations are carried out based on this equation of motion.

B. Clock-driven Leg Controller

The robot has a simple clock-driven, open-loop gait. The joints of the robot are manipulated by motors using a proportional-derivative (PD) controller. Specifically, the leg joints are controlled by incorporating periodic desired angles, while the coupler joints are controlled without using such desired angles. Therefore, in that sense, the coupler joints act like a passive spring with a damper.

To design the periodic desired angles of the leg joints, we first introduce Oscillator i, j ($i = 1, \ldots, 6$, $j = 1, 2$) for Leg j of Module i. Oscillator i, j has phase ϕ_i^j whose angular velocity is constant. Second, we design nominal trajectory η_i^j

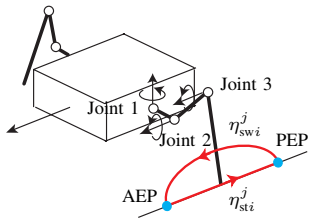

Fig. 2. Nominal trajectory of the leg

$(i = 1, \ldots, 6,\ j = 1, 2)$ of the tip of Leg j of Module i in the sagittal plane as a function of phase ϕ_i^j, that is, $\eta_i^j = \eta_i^j(\phi_i^j)$. Trajectory η_i^j is expressed in the body of Module i and consists of trajectories η_{swi}^j for the swing phase and η_{sti}^j for the stance phase $(i = 1, \ldots, 6,\ j = 1, 2)$ (see Fig. 2). Trajectory η_{swi}^j is composed of half of an elliptic curve that includes the anterior extreme position (AEP) and the posterior extreme position (PEP). Note that the distance between points AEP and PEP implies nominal stride s. Trajectory η_{sti}^j is comprised of a straight line that also involves points AEP and PEP. During the stance phase, the tip of the leg moves at constant speed $v(= s/(\beta\tau))$ with respect to the body in the opposite walking direction, where τ is the nominal step cycle and β indicates the nominal duty ratio that expresses the ratio between the nominal stance phase duration and the nominal step cycle. Note that since the tip of the leg is constrained on the ground during the stance phase, the body moves in the walking direction at nominal locomotion speed v with respect to the ground. In light of the above description, trajectory η_i^j is given by (see details in [2])

$$\eta_i^j(\phi_i^j) = \begin{cases} \eta_{\mathrm{swi}}^j(\phi_i^j) & 0 \le \phi_i^j < \phi_{\mathrm{a}} \\ \eta_{\mathrm{sti}}^j(\phi_i^j) & \phi_{\mathrm{a}} \le \phi_i^j < 2\pi \end{cases} \quad i = 1, \ldots, 6,\ \ j = 1, 2 \tag{2}$$

where $\phi_{\mathrm{a}} = 2\pi(1 - \beta)$, which indicates the nominal phase value at point AEP (0 at point PEP). When trajectory η_i^j is on point PEP at $t = 0$, it arrives at point AEP at $t = (1 - \beta)\tau$ through the swing phase and turns into the stance phase. It then reaches point PEP at $t = \tau$ and returns to the swing phase. Finally, based on the inverse kinematics, we obtain desired angles $\hat{\theta}_{ik}^j$ $(i = 1, \ldots, 6,\ j = 1, 2,\ k = 1, 2, 3)$ of Joint k of Leg j of Module i as the function of phase ϕ_i^j.

In numerical simulations, the contralateral legs on each module and the unilateral legs on adjacent modules move out of phase with each other. That is, the phases of the oscillators have relationships such that $\phi_i^1 - \phi_i^2 = \pi$ $(i = 1, \ldots, 6)$ and $\phi_i^j - \phi_{i+1}^j = \pi$ $(i = 1, \ldots, 5,\ j = 1, 2)$. Nominal stride s, duty ratio β, and step cycle τ of each leg are set to 5 cm, 0.5, and 0.5 s, respectively. In this case, nominal locomotion speed v becomes equivalent to 0.2 m/s. Point AEP of both legs of each module is located 4.5 cm ahead and 7.5 cm outside of the center of the module in the nominal direction of locomotion.

III. Dynamic Properties

A. Transition from a Straight to a Meandering Walk

This robot has interesting and essential characteristics in locomotion. Since the couplers act like a spring with a damper, the robot is able to achieve a straight walk as long as it moves its legs in a similar manner. However, it is clear that when we decrease the feedback gains of the couplers' yaw joints, a meandering walk appears beyond a critical point without incorporation of any oscillatory inputs into the couplers. This means that the robot's walking motion naturally varies according to changes in its mechanical properties.

TABLE I

Physical Parameters of the Multi-Legged Modular Robot

Link	Parameter	Value
Body	Mass [kg]	0.6
	Length [m]	0.2
	Width [m]	0.08
	Inertia [$\times 10^{-3}$kgm^2]	3.1
Link 1	Mass [kg]	0.02
	Length [m]	0.015
Link 2	Mass [kg]	0.03
	Length [m]	0.045
Link 3	Mass [kg]	0.05
	Length [m]	0.15
Motor	Gear ratio	100
	Rotor inertia [$\times 10^{-7}$kgm^2]	9.7

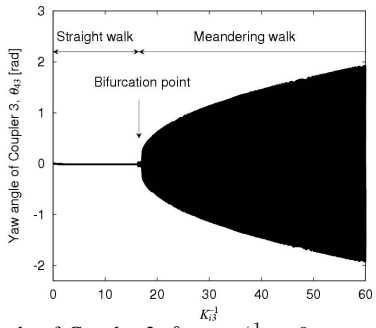

Fig. 3. Yaw angle of Coupler 3, θ_{43}, at $\phi_1^1 = 0$ versus the reciprocal of gain parameter K_{i3}^{-1}

Here, we present detailed results obtained through numerical simulations. Table I displays the physical parameters of the multi-legged modular robot used in the numerical simulations. The damping coefficient of the ground in the horizontal direction is set to 19.6 Ns/m. To change the mechanical features of the robot, we parameterize proportional feedback gain K_{i3} and derivative feedback gain D_{i3} $(i = 2, \ldots, 6)$ of the couplers' yaw joints by using parameter f

$$K_{i3} = K_0(2\pi f)^2,\ D_{i3} = 2K_0\zeta(2\pi f) \quad i = 2, \ldots, 6 \tag{3}$$

where K_0 and ζ are set to 0.0097 and 0.8, respectively. Note that for other joints high feedback gains are used and parameter f is set to 10 (e.g. $K_{i1,2}^{-1} = 0.0261$, $i = 2, \ldots, 6$). Also note that this change of the feedback gains indicates a change in the joints' compliance. Figure 3 shows yaw angle θ_{43} of Coupler 3 at $\phi_1^1 = 0$ with respect to the reciprocal of gain parameter K_{i3}^{-1}, revealing that undulatory motion is excited over a bifurcation point. This figure also implies that since the angles are plotted with respect to each step cycle of the leg motion, this meandering motion is not synchronized with the leg motion. Therefore, it has an independent frequency (see details in Fig. 7(c) shown below). Figures 4(a) and (b) are snapshots of the front and overhead views, respectively, of the walking motion using $K_{i3}^{-1} = 21$, showing that wavy motion appears.

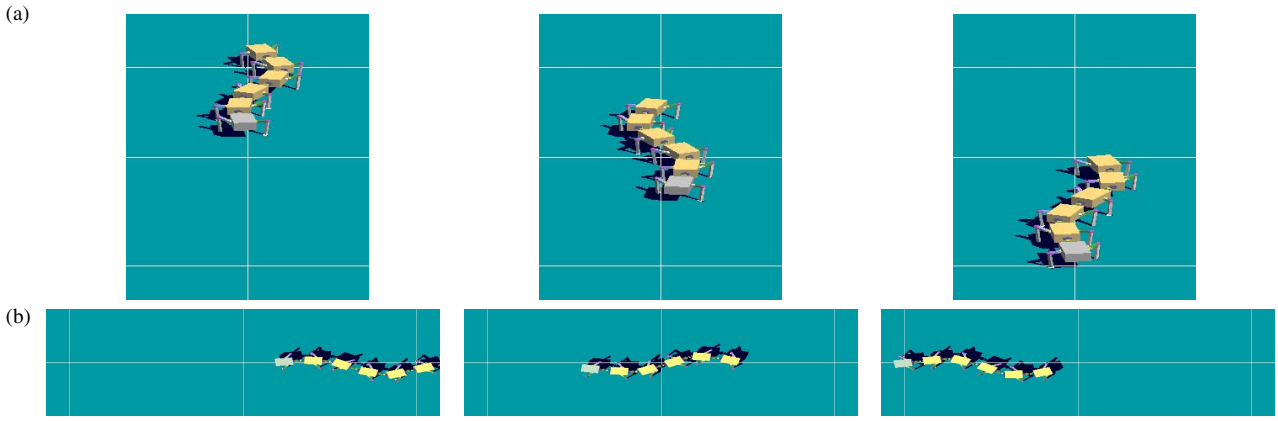

Fig. 4. Meandering motion. (a) Front view. (b) Overhead view.

B. Investigation of the Transition Mechanism

As shown above, a straight walk naturally turns into a meandering walk by changes in the mechanical characteristics. This transition is expected to imply that a straight walk is destabilized and that undulatory motion is excited due to a Hopf bifurcation. In this section we analyze its mechanism in detail.

To investigate it, we simplify the robot model by assuming the following for its straight walk [32]: 1) the up-and-down, roll, and pitch motions of the robot are sufficiently small with respect to other motions and can be ignored; 2) the leg mass is too small in comparison to the body mass and the leg joints completely follow the kinematically designed trajectories as shown in Fig. 2; and 3) the robot walks at constant speed v. Figure 5 shows an overhead view of this simplified model. Note that the legs receive the force from the ground, only when they are in the stance phase.

Under these assumptions, state variable $q \in \mathbb{R}^8$ is redefined as $q^{\mathrm{T}} = [\, x_1\, x_2\, \theta_{13} \cdots \theta_{63}\,]$. Then, we define state $\xi \in \mathbb{R}^{16}$ as $\xi^{\mathrm{T}} = [\, \dot{q}^{\mathrm{T}}\, q^{\mathrm{T}}\,]$. In a straight walk, state ξ can be written as $\xi_{\mathrm{str}}^{\mathrm{T}} = [\, v\ 0 \cdots 0\ vt + x_{10}\ 0 \cdots 0\,]$, where x_{10} is the state of x_1 at $t = 0$. Perturbed state $\xi \in \mathbb{R}^{16}$ from a straight walk is defined as $\xi = \xi_{\mathrm{str}} + \delta\xi$, where $\delta\xi \in \mathbb{R}^{16}$ is the perturbation. By contracting equation of motion (1) and then linearizing it around state ξ_{str}, we obtain

$$\dot{\delta\xi} = A(t)\delta\xi \tag{4}$$

where matrix $A(t) \in \mathbb{R}^{16\times16}$ is periodic and $A(t+\tau) = A(t)$ for step cycle τ of the leg motion.

Based on the Floquet theory, we analyze the stability of a straight walk, where for the simplified model the mass and inertial of each module are set to 0.8 kg and 4.2×10^{-3} kgm^2, respectively. Figures 6(a) and (b) show the trajectories of the Floquet (characteristic) exponents while the feedback gains of the yaw joints of the couplers change. Specifically, Fig. 6(a) shows all the trajectories of the Floquet exponents, revealing that a Hopf bifurcation occurs by crossing the imaginary axis. Displayed circles indicate all the 16 Floquet exponents when the Hopf bifurcation takes place, where red circles correspond to the Hopf bifurcation. Figure 6(b) shows trajectories in detail by focusing on the vicinity of the imaginary axis.

Next, we verify whether this Hopf bifurcation actually explains the transition from a straight to a meandering walk ob-

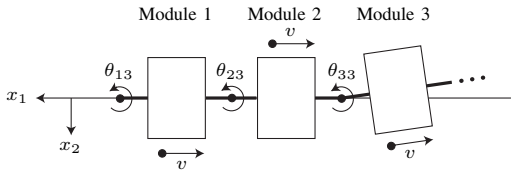

Fig. 5. Overhead view of the simplified model

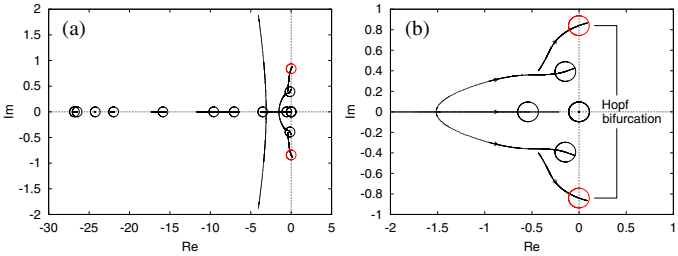

Fig. 6. Floquet exponents. (a) Trajectories of all the Floquet exponents. (b) Enlarged detail.

tained in numerical simulations. Figure 7 shows a comparison between the results of the numerical simulation and Floquet analysis, where the obtained meandering motion is used for the numerical simulation and the eigenvector corresponding to the destabilized Floquet exponent is used for the Floquet analysis. In particular, Figs. 7(a), (b), and (c) illustrate the phase difference with respect to angle θ_{13}, the amplitude ratio between the angles, and the period of the meandering motion, respectively. Although the simplification causes some errors, these results are almost the same in quality and quantity. Therefore, we conclude that the transition from a straight to a meandering walk is caused by a Hopf bifurcation due to the change of the couplers' yaw joints.

IV. Turning Maneuver using Dynamic Properties

Dynamic characteristics such as stability must greatly affect the maneuverability and agility of locomotion. Schmitt and Holmes [26], [27] simply modeled the hexapod walking of a cockroach, which has marvelous agility, and analytically demonstrated that it successfully achieves a quick turn by virtue of destabilizing its straight walk through changing its dynamic features.

In this section, we investigate the relationship between the dynamic features and maneuverability of the robot. To clarify this relationship, we have the robot pursue a target moving

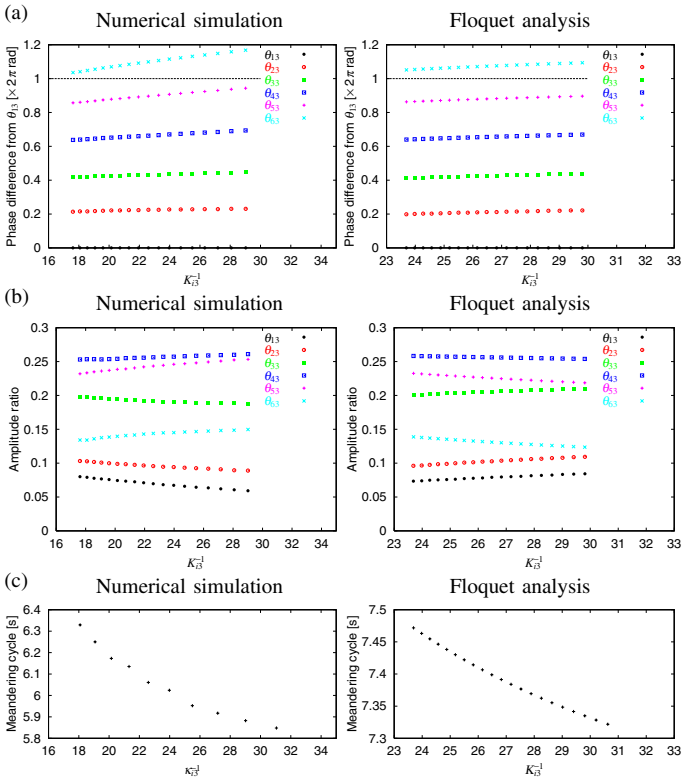

Fig. 7. Comparison between numerical and analytical results. (a) Phase difference with respect to θ_{13}. (b) Amplitude ratio between angles. (c) Period of meandering motion.

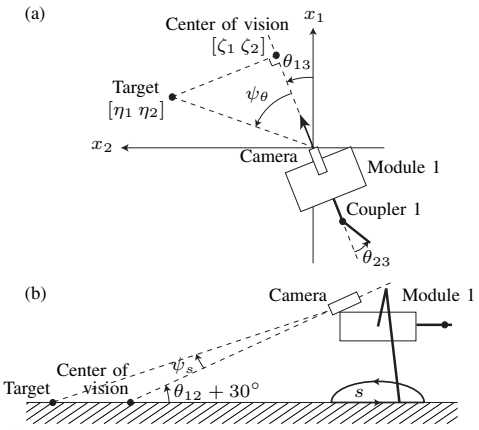

Fig. 8. Target pursuit. (a) Direction ψ_θ. (b) Distant angle ψ_s.

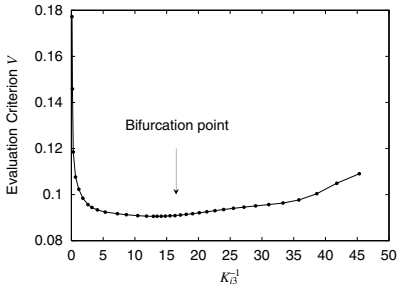

Fig. 9. Evaluation criterion V versus the reciprocal of gain parameter K_{i3}^{-1}

across the floor. A camera is attached to the head of Module 1 whose elevation angle is $-30°$. From the visual image taken by the camera, the robot can obtain direction angle ψ_θ and distance angle ψ_s (see Figs. 8(a) and (b)). The center of vision is the intersection point between the ground and the visual line of the camera, whose position is expressed by $[\,\eta_1\ \eta_2\,]$ on the floor. The position of the target is $[\,\zeta_1\ \zeta_2\,]$. The sampling frequency of the visual information is set to be 20 Hz. By using information ψ_θ and ψ_s, the robot attempts to follow the moving target.

To manipulate the walking direction, input torque τ_{13} at the yaw joint of Coupler 1 is activated by incorporating the desired angle regarding visual information ψ_θ, given by

$$\tau_{23} = -K_{23}(\theta_{23} + \psi_\theta) - D_{23}\dot{\theta}_{23} \tag{5}$$

where feedback gains K_{23} and D_{23} are fixed and parameter f in Eq. (3) is set to 1.0 for them. The aim of this control is to point the first module in the direction of the target and then make the other modules follow the first module through their passive connections. To approach the target, by using visual information ψ_s, stride s is determined by

$$s = K_s\psi_s \tag{6}$$

where K_s is set to 0.191 m/rad and stride s is limited with a saturation at ± 5 cm.

In the task of pursuing the target, the target moves along a trajectory composed of connected straight lines at a constant speed 0.18 m/s (see Fig. 10). We carry out this task with respect to feedback gains K_{i3} and D_{i3} of the couplers' yaw joints except for Coupler 1 ($i = 3, \ldots, 6$), given in Eq. (3). To examine the agility of locomotion, we employ evaluation criterion V, which represents the mean square error between the target and center of vision, given by

$$V = \frac{1}{\tau_{\text{task}}}\int_0^{\tau_{\text{task}}} \sqrt{(\eta_1-\zeta_1)^2 + (\eta_2-\zeta_2)^2}\, dt \tag{7}$$

where τ_{task} is the time interval to execute this task (set to 80 s). Figure 9 shows evaluation criterion V with respect to the reciprocal of gain parameter K_{i3}^{-1}. Figures 10(a) and (b) show the trajectories of the target and center of vision , and of the target and Module 1, respectively, during the target pursuit, especially with respect to $K_{i3}^{-1} = 0.1$, 16, and 45. These figures show that the robot achieves high maneuverability and agility by using the feedback gain around the bifurcation point where a straight walk turns into a meandering one. When the feedback gains are larger than the bifurcation point, evaluation criterion V also larger. This reflects that the robot is unable to obtain sufficient maneuverability, which makes the modules behind Module 1 unable to smoothly follow Module 1. When the feedback gains are smaller than the bifurcation point, evaluation criterion V also larger. It is partly because the undulatory motion is excited during target pursuit. These results imply that the decrease in stability during a straight walk, due to a reduction in the strength of the connection between the modules, helps the robot to efficiently accomplish this task. In other words, the robot appears to achieve its maneuverability and agility by virtue of changes in the dynamic characteristics.

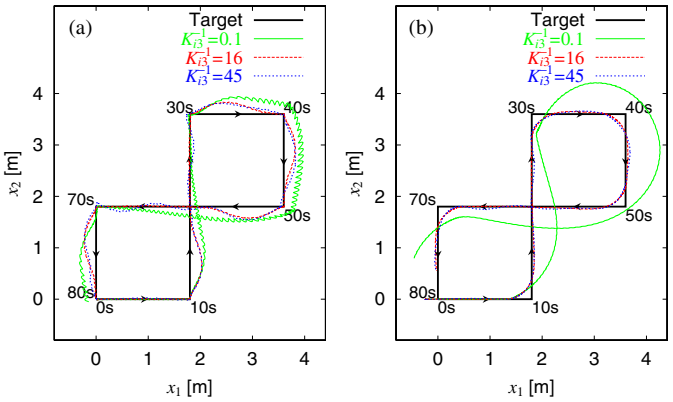

Fig. 10. Target pursuit. (a) Trajectories of the target and the vision center. (b) Trajectories of the target and Module 1.

V. Conclusion

In this paper, we dealt with locomotion of a six-module, twelve-legged robot. In particular, we showed that a straight walk by this robot naturally changes into a meandering walk by changes in the compliance of the yaw joints between the modules without incorporation of any oscillatory inputs. Based on the Floquet theory, we first clarified that this transition reflects that a straight walk is destabilized and undulatory motion is excited due to a Hopf bifurcation. Then, we investigated the role of this dynamic property in achieving maneuverability and agility, conducting an experiment in which the robot pursued a target moving across the floor. By using the proposed simple controller, the robot accomplished the task and performed high maneuverability and agile motions by making the most of the dynamic characteristics inherent in it.

Acknowledgment

This paper is supported in part by Center of Excellence for Research and Education on Complex Functional Mechanical Systems (COE program of the Ministry of Education, Culture, Sports, Science and Technology, Japan) and by a Grant-in-Aid for Scientific Research on Priority Areas “Emergence of Adaptive Motor Function through Interaction between Body, Brain and Environment” from the Japanese Ministry of Education, Culture, Sports, Science and Technology.

References

[1] R. Altendorfer, D.E. Koditschek, and P. Holmes, *Stability analysis of a clock-driven rigid-body SLIP model for RHex*, Int. J. Robot. Res., 23(10-11):1001–1012, 2004.

[2] S. Aoi and K. Tsuchiya, *Locomotion control of a biped robot using nonlinear oscillators*, Auton. Robots, 19(3):219–232, 2005.

[3] S. Aoi and K. Tsuchiya, *Self-stability of a simple walking model driven by a rhythmic signal*, Nonlinear Dyn., in press.

[4] S. Aoi and K. Tsuchiya, *Stability analysis of a simple walking model driven by an oscillator with a phase reset using sensory feedback*, IEEE Trans. Robotics, 22(2):391–397, 2006.

[5] J.-D. Boissonnat, O. Devillers, and S. Lazard, *Motion planning of legged robots*, SIAM J. Comput., 30(1):218-246, 2000.

[6] A. Castano, W.-M. Shen, and P. Will, *CONRO: Towards deployable robots with inter-robot metamorphic robots*, Auton. Robots, 8:309–324, 2000.

[7] J.G. Cham, J.K. Karpick, and M.R. Cutkosky, *Stride period adaptation of a biomimetic running hexapod*, Int. J. Robot. Res., 23(2):141–153, 2004.

[8] A. Crespi, A. Badertscher, A. Guignard, and A.J. Ijspeert, *AmphiBot I: An amphibious snake-like robot*, Robot. Auton. Syst., 50(4):163–175, 2005.

[9] K.S. Espenschied, R.D. Quinn, R.D. Beer, and H.J. Chiel, *Biologically based distributed control and local reflexes improve rough terrain locomotion in a hexapod robot*, Robot. Auton. Syst., 18(1-2):59–64, 1996.

[10] T. Fukuda and Y. Kawauchi, *Cellular robotic system (CEBOT) as one of the realization of self-organizing intelligent universal manipulator*, Proc. IEEE Int. Conf. on Robot. Autom., pp. 662–667, 1990.

[11] Y. Fukuoka, H. Kimura, and A. Cohen, *Adaptive dynamic walking of a quadruped robot on irregular terrain based on biological concepts*, Int. J. Robot. Res., 22(3-4):187–202, 2003.

[12] R.J. Full, T. Kubow, J. Schmitt, P. Holmes, and D. Koditschek, *Quantifying dynamic stability and maneuverability in legged locomotion*, Integ. and Comp. Biol., 42:149–157, 2002.

[13] M. Garcia, A. Chatterjee, A. Ruina, and M. Coleman, *The simplest walking model: Stability, complexity, and scaling*, ASME J. Biomech. Eng., 120(2):281–288, 1998.

[14] H. Geyer, A. Seyfarth, and R. Blickhan, *Spring-mass running: simple approximate solution and application to gait stability*, J. Theor. Biol., 232(3):315–328, 2005.

[15] R. Ghigliazza, R. Altendorfer, P. Holmes, and D.E. Koditschek, *A simply stabilized running model*, SIAM J. Applied Dynamical Systems, 2(2):187–218, 2003.

[16] Y. Go, X. Yin, and A. Bowling, *Navigability of multi-legged robots*, IEEE/ASME Trans. Mechatronics, 11(1):1–8, 2006.

[17] S. Grillner, *Neurobiological bases of rhythmic motor acts in vertebrates*, Science, 228:143–149, 1985.

[18] S. Inagaki, H. Yuasa, T. Suzuki, and T. Arai, *Wave CPG model for autonomous decentralized multi-legged robot: Gait generation and walking speed control*, Robot. Auton. Syst., 54(2):118–126, 2006.

[19] A. Ishiguro, K. Ishimaru, K. Hayakawa, and T. Kawakatsu, *How should control and body dynamics be coupled? - A robotic case study -*, Proc. IEEE/RSJ Int. Conf. on Intell. Robots Syst., pp. 1727–1732, 2003.

[20] D.L. Jindrich and R.J. Full, *Many-legged maneuverability: Dynamics of turning in hexapods*, J. Exp. Biol., 202:1603–1623, 1999.

[21] S. Mori, *Integration of posture and locomotion in acute decerebrate cats and in awake, free moving cats*, Prog. Neurobiol., 28:161–196, 1987.

[22] J. Nakanishi, J. Morimoto, G. Endo, G. Cheng, S. Schaal, and M. Kawato, *Learning from demonstration and adaptation of biped locomotion*, Robot. Auton. Syst., 47(2-3):79–91, 2004.

[23] G.N. Orlovsky, T. Deliagina, and S. Grillner, Neuronal control of locomotion: from mollusc to man, *Oxford University Press*, 1999.

[24] I. Poulakakis, J.A. Smith, and M. Buehler, *Modeling and experiments of untethered quadrupedal running with a bounding gait: The Scout II Robot*, Int. J. Robot. Res., 24(4):239–256, 2005.

[25] U. Saranli, M. Buehler, and D.E. Koditschek, *RHex: A simple and highly mobile hexapod robot*, Int. J. Robot. Res., 20(7):616–631, 2001.

[26] J. Schmitt and P. Holmes, *Mechanical models for insect locomotion: dynamics and stability in the horizontal plane I. Theory*, Biol. Cybern., 83:501–515, 2000.

[27] J. Schmitt and P. Holmes, *Mechanical models for insect locomotion: dynamics and stability in the horizontal plane - II. Application*, Biol. Cybern., 83:517–527, 2000.

[28] G. Taga, Y. Yamaguchi, and H. Shimizu, *Self-organized control of bipedal locomotion by neural oscillators*, Biol. Cybern., 65:147–159, 1991.

[29] K. Takakusaki, T. Habaguchi, J. Ohtinata-Sugimoto, K. Saitoh, and T. Sakamoto, *Basal ganglia efferents to the brainstem centers controlling postural muscle tone and locomotion; A new concept for understanding motor disorders in basal ganglia dysfunction*, Neuroscience, 119:293–308, 2003.

[30] T. Takuma, K. Hosoda, and M. Asada, *Walking stabilization of biped with pneumatic actuators against terrain changes*, Proc. IEEE/RSJ Int. Conf. on Intell. Robots Syst., pp. 2775–2780, 2005.

[31] K. Tsuchiya, S. Aoi, and K. Tsujita, *Locomotion control of a multi-legged locomotion robot using oscillators*, Proc. IEEE Int. Conf. on Syst., Man, Cybern., TA2G2, 2002.

[32] K. Tsuchiya, S. Aoi, and K. Tsujita, *A turning strategy of a multi-legged locomotion robot*, Proc. 2nd Int. Symp. on Adaptive Motion of Animals and Machines, ThP-I-1, 2003.

[33] H. Wagner and R. Blickhan, *Stabilizing function of skeletal muscles: an analytical investigation*, J. Theor. Biol., 199:163–179, 1999.

[34] M. Wisse, A.L. Schwab, R.Q. van der Linde, and F.C.T. van der Helm, *How to keep from falling forward: elementary swing leg action for passive dynamic walkers*, IEEE Trans. Robotics, 21(3):393–401, 2005.

[35] M. Yim, Y. Zhang, K. Roufas, D. Duff, and C. Eldershaw, *Connecting and disconnecting for chain selfreconfiguration with polybot*, IEEE/ASME Trans. Mechatronics, 7(4):442–451, 2002.

[36] E. Yoshida, S. Murata, A. Kamimura, K. Tomita, H. Kurokawa, and S. Kokaji, *A self-reconfigurable modular robot: Reconfiguration planning and experiments*, Int. J. Robot. Res., 21(10):903–916, 2002.